

As shown in Fig. 1, an RMP consists of two components, a “leg” that joins the CoP and the CoM, and an ellipsoidal “body” – the abstracted reaction mass – that characterizes the generalized inertia of the entire robot projected at the CoM. As the robot moves in space, so does the RMP, resulting in a continuous movement of the CoP and CoM. All limb movements of the robot affect its centroidal moment of inertia, which is captured by the changing shape, size and orientation of the ellipsoidal reaction mass.

II. GENERATING THE RMP MODEL OF A HUMANOID

We generate the RMP model of a humanoid by developing the concept of generalized inertia of an articulated chain. In this section we derive the necessary equations starting from a single rigid body to finally exploit the concept of composite rigid body (CRB) inertia. In Section III we outline a mechanical realization of the RMP.

A. Generalized inertia of single rigid body

The *generalized inertia* of a rigid body \mathbf{I} with respect to a body-fixed coordinate frame has the following structure

$$\mathbf{I} = \begin{bmatrix} \bar{\mathbf{I}} & m[\mathbf{r}] \\ -m[\mathbf{r}] & m\mathbf{E} \end{bmatrix}, \quad (1)$$

where m is the mass, $\bar{\mathbf{I}} \in \mathbb{R}^{3 \times 3}$ is the rotational inertia matrix, $\mathbf{r} \in \mathbb{R}^3$ is the position of the CoM¹, and \mathbf{E} is the 3×3 identity matrix. $\bar{\mathbf{I}}$ and \mathbf{I} are symmetric positive definite matrices.

Let $\mathbf{T} = \begin{bmatrix} \mathbf{R} & \mathbf{p} \\ 0 & 1 \end{bmatrix} \in \text{SE}(3)$ denote the homogeneous transformation matrix of the body frame with respect to a spatial frame $\{s\}$. Then the *generalized velocity* \mathbf{V} of the rigid body with respect to the body frame is given by

$$\mathbf{V} = \mathbf{T}^{-1}\dot{\mathbf{T}} = \begin{bmatrix} [\mathbf{w}] & \mathbf{v} \\ 0 & 0 \end{bmatrix} \in \text{se}(3)$$

where \mathbf{w} and \mathbf{v} are its angular and linear velocities. \mathbf{V} will also be written as $\mathbf{v} = (\mathbf{w}^T, \mathbf{v}^T)^T$ for convenience. Subsequently, the *generalized momentum* of the rigid body is

$$\mathbf{h} = (\mathbf{k}^T, \mathbf{l}^T)^T = \mathbf{I}\mathbf{v} \in \text{se}^*(3)$$

where \mathbf{k} and \mathbf{l} are the angular and linear momenta.

The generalized velocity \mathbf{V} with respect to $\{s\}$ is given by ${}^s\mathbf{V} = \text{Ad}_{\mathbf{T}}\mathbf{V} = \mathbf{T}\mathbf{V}\mathbf{T}^{-1}$.² The *adjoint mapping* $\text{Ad}_{\mathbf{T}} : \text{se}(3) \rightarrow \text{se}(3)$, also known as spatial motion transform, can be written as

$$\text{Ad}_{\mathbf{T}}\mathbf{V} = \begin{bmatrix} \mathbf{R} & 0 \\ [\mathbf{p}]\mathbf{R} & \mathbf{R} \end{bmatrix} \begin{pmatrix} \mathbf{w} \\ \mathbf{v} \end{pmatrix}.$$

¹ $[\mathbf{r}]$ is the skew-symmetric matrix representation of \mathbf{r} ; i.e., $[\mathbf{r}_1]\mathbf{r}_2 = \mathbf{r}_1 \times \mathbf{r}_2$.

²Left superscript s indicates the symbol is expressed in a spatial frame $\{s\}$. Likewise, we will use left superscript 0 and g to indicate a spatial frame that coincides with the base frame and the one located at CoM of the humanoid robot respectively. No left superscript is used when a symbol is expressed in the body frame.

The generalized momentum with respect to $\{s\}$ is ${}^s\mathbf{h} = \text{Ad}_{\mathbf{T}^{-1}}^*\mathbf{h}$, where *dual adjoint mapping* $\text{Ad}_{\mathbf{T}}^* : \text{se}^*(3) \rightarrow \text{se}^*(3)$ is defined as

$$\text{Ad}_{\mathbf{T}}^* = \begin{bmatrix} \mathbf{R} & 0 \\ [\mathbf{p}]\mathbf{R} & \mathbf{R} \end{bmatrix}^T.$$

Finally, by exploiting the equality of the kinetic energy in two different frames, we can derive the coordinate transformation of the generalized inertia;

$${}^s\mathbf{I} = \text{Ad}_{\mathbf{T}^{-1}}^*\mathbf{I}\text{Ad}_{\mathbf{T}^{-1}}. \quad (2)$$

One can find more details on Lie group theoretic approach on rigid body kinematics from [8].

B. CRB inertia of a humanoid robot

We assume that a humanoid robot model consists of $n + 1$ links with the base link, usually the pelvis, indexed as 0. $\Theta = (\mathbf{T}_0, \mathbf{q})$ denotes the generalized coordinates of the humanoid robot, where $\mathbf{T}_0 \in \text{SE}(3)$ is the transformation matrix of the body frame of the base link (*base frame* hereafter.) and $\mathbf{q} = (q_1, \dots, q_n)^T \in \mathbb{R}^n$ is the joint angle vector of the robot. Subsequently, $\dot{\Theta}$ denotes the body velocity of the base frame and joint velocities, i.e., $(\mathbf{V}_0, \dot{\mathbf{q}})$, where $\mathbf{V}_0 = \mathbf{T}_0^{-1}\dot{\mathbf{T}}_0$.

\mathbf{T}_i denotes the transformation matrix from the spatial frame to the body frame of link i , and $\mathbf{G}_i = \mathbf{T}_0^{-1}\mathbf{T}_i$ is the transformation matrix from the base frame to link i . Note that \mathbf{G}_i does not depend on \mathbf{T}_0 and is entirely determined by \mathbf{q} . We assume that, except for the base link, each link is connected to its parent link by a 1-DOF joint. Then $\mathbf{T}_i = \mathbf{T}_{p_i}\mathbf{H}_i e^{\mathbf{S}_i q_i}$ holds for $i > 0$ where p_i is the parent link of the link i , \mathbf{H}_i is the transformation from p_i to i at $q_i = 0$, and $\mathbf{S}_i \in \text{se}(3)$ is the screw parameter of the joint.

We define the *link Jacobian* \mathbf{J}_i of a link i similar to the manipulator Jacobian as follows;

$$\mathbf{J}_i = [\text{Ad}_{\mathbf{G}_i^{-1}}, \mathbf{J}_{i,q}] \quad (3)$$

$$\mathbf{J}_{i,q} = [J_{i,1}, \dots, J_{i,n}] \in \mathbb{R}^{6 \times n} \quad (4)$$

where $J_{i,j} = \mathbf{T}_i^{-1}(\partial\mathbf{T}_i/\partial q_j) = \mathbf{G}_i^{-1}(\partial\mathbf{G}_i/\partial q_j)$. $\text{Ad}_{\mathbf{G}_i^{-1}}$ and $\mathbf{J}_{i,q}$ are the Jacobians due to the change of the base frame and joint angles respectively. $J_{i,j}$ can be computed recursively as follows;

$$J_{i,j} = \text{Ad}_{\mathbf{H}_i e^{\mathbf{S}_i q_i}}^{-1} J_{p_i,j} + \mathbf{S}_i \delta_{i,j} \quad \text{for } i = 1 \dots n \quad (5)$$

where $J_{0,j} = 0$ and $\delta_{i,j}$ is the Kronecker delta function.

Using the link Jacobian, we can decompose the velocity of $\{i\}$ into the sum of the velocity due to the base link and the one due to the joint velocities;

$$\mathbf{v}_i = \mathbf{J}_i \dot{\Theta} = \text{Ad}_{\mathbf{G}_i^{-1}}\mathbf{v}_0 + \mathbf{J}_{i,q}\dot{\mathbf{q}}. \quad (6)$$

The generalized momentum \mathbf{h} of the humanoid robot is the sum of generalized momentum of each link. The one

with respect to the base frame ³ is

$${}^0\mathbf{h} = \sum_i {}^0\mathbf{h}_i = \sum_i {}^0\mathbf{I}_i {}^0\mathbf{v}_i \quad (7)$$

$$= {}^0\mathbf{I}\mathbf{v}_0 + \sum_i \text{Ad}_{\mathbf{G}_i}^* \mathbf{I}_i \mathbf{J}_{i,q} \dot{\mathbf{q}} \quad (8)$$

$$= {}^0\mathbf{I}(\mathbf{v}_0 + \mathbf{A}\dot{\mathbf{q}}) \quad (9)$$

where ${}^0\mathbf{I} = \sum \text{Ad}_{\mathbf{G}_i}^* \mathbf{I}_i \text{Ad}_{\mathbf{G}_i} = \sum {}^0\mathbf{I}_i$ is the *CRB inertia* [22] expressed in the base frame and $\mathbf{A}(\mathbf{q})$ is the so-called *mechanical connection* [9]. The CRB inertia of a humanoid robot is its instantaneous generalized inertia, assuming that all of its joints are frozen. It has the same structure as the generalized inertia of a single rigid body (Eq. 1). CRB inertia is identical to the so-called locked inertia, used in geometric mechanics[9]. As can be seen in (9), the CRB inertia contributes directly to the generalized momentum via the mechanical connection.

While the CRB inertia can be expressed with respect to any frame, the one at CoM is particularly interesting since it is related to the centroidal angular momentum. Hence we use ${}^g\mathbf{I}$ in the RMP model.

C. Equipomental ellipsoids

The association of the rigid body inertia to an ellipsoid is well known and has been thoroughly exploited in physics and engineering [10]. In a similar fashion, we determine the ellipsoid associated with the centroidal CRB inertia of an articulated chain. Instead of using the kinetic energy ellipsoid, which is traditionally described with an inertia, we derive the *equipomental* ellipsoid corresponding to a CRB inertia. Two inertias are said to be equipomental if their moments of inertia about any arbitrary axis are equal [11]. The equipomental ellipsoid of a rigid body is an ellipsoid with a uniform density set as the mean density of the body and having the same rotational inertia about any arbitrary axis as that of the rigid body. Kinetic energy ellipsoid characterizes the torque needed to rotate the body *about* an axis whereas the equipomental ellipsoid reflects the mass distribution *along* an axis.

Let $(\sigma_1, \sigma_2, \sigma_3)$ denote the eigenvalues of the rotational inertia, and (a_1, a_2, a_3) denote the semi-axes of the equipomental ellipsoid. From the relationships $\sigma_1 = \frac{2}{5}ma_2a_3$, $\sigma_2 = \frac{2}{5}ma_1a_3$, $\sigma_3 = \frac{2}{5}ma_1a_2$, and $m = \frac{4}{3}\pi a_1a_2a_3\rho$, where ρ is the mean density, we can derive the following:

$$a_i = \frac{(\sigma_1 \sigma_2 \sigma_3)^{2/5}}{\sigma_i (8\pi\rho/15)^{1/5}} \quad \text{for } i = 1, 2, 3$$

D. Simulation results

We used Webots [12], a commercial simulation software, and developed additional code to establish a platform that continuously maps a given motion of a humanoid into its corresponding RMP. The process involves the computation of 1) CoM, 2) CoP, and 3) CRB Inertia about CoM, using robot kinematic and dynamic parameters, as well as motion data. We simulated the Fujitsu HOAP2 biped model, for

which the parameters for some dramatic movements are available [13].

Fig. 2 shows snapshots of HOAP2 executing Sumo-style movements. Notice the significant changes in the shape, size and orientation of the reaction mass ellipsoid⁴ as the robot moves through different phases of its motion. Since the robot→RMP is a mapping to a lower dimension, different poses of the robot, at least theoretically, may get mapped to the same RMP.

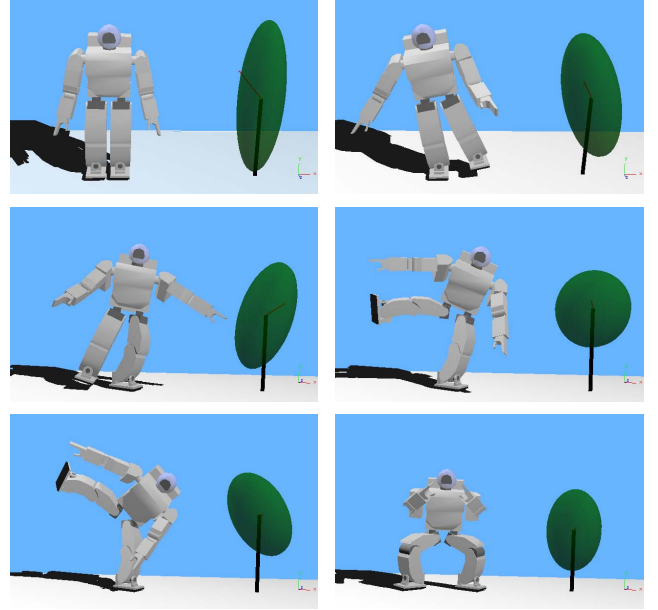


Fig. 2. Snapshots of HOAP2 robot performing Sumo-style motion superposed with corresponding RMP models. The reaction mass geometry undergoes significant changes during this motion.

III. PROPERTIES AND PARAMETERS OF RMP

We have now seen how a humanoid robot can be reduced to an RMP. In this section we will discuss the realization of a mechanical model of the RMP.

A. Description of RMP

The reaction wheel, which is also called inertia wheel, is one of a number of standard momentum exchange devices that are used to control satellite orientation [14]. An actuated reaction wheel attached to a rigid rod becomes a reaction wheel pendulum which has also been studied [15], [16], [17]. The present work can be identified with that of [18], [19], where the benefit of a reaction mass feature of the humanoid as a mean to stabilize lateral biped dynamics is indicated. The current work is closest in spirit to the recently introduced inverted pendulum model with angular momentum properties (AMPM) [20], [4]. We seek to propose a physical model characterizing angular momentum.

The RMP *mathematical* model discussed here is not to be confused with the actual placement of a *physical* reaction mass device for the control of humanoid balance, as was done in [21].

³More precisely, a spatial frame that coincides with the base frame.

⁴Reaction mass ellipsoid and CRB inertia ellipsoid are synonymous

The 3D reaction mass has continuously variable inertia. At any given configuration of the robot, the CRB inertia can be reduced to an ellipsoid. This is modeled, as shown in Fig. 3(a) by three pairs of point masses linearly actuated along the three principal orthogonal directions of the ellipsoid. Along each axis k , the distance between the point masses is $2r_k$. The masses of each pair are always equidistant from the ellipsoid center. The CoM of the ellipsoid is therefore always fixed at its center. The six point mass can have equal masses, i.e., $m = M/6$, so that they sum up to total mass of the humanoid robot. The distance between the masses depends on its corresponding rotational inertia, as each axis generates a moment of inertia mr_k^2 .

The radial movement of the point masses only affect the shape and size of the ellipsoid. When $r_k = 0$ for $k = 1, 2, 3$ the ellipsoid reduces to a point mass and the RMP reduces to a 3D inverted pendulum. The list of all eleven generalized coordinates and nine generalized forces are listed in Table. I.

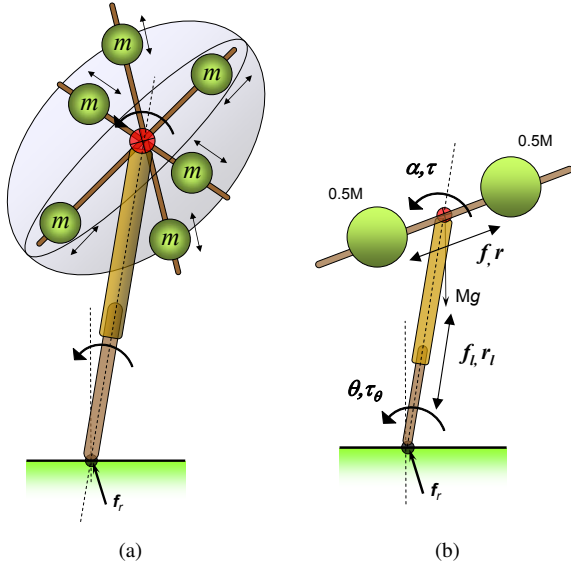


Fig. 3. (a) Conceptual mechanical realization of the 3D RMP. The ellipsoid can be reduced to three pairs of equal point masses at different radial distances that are radially actuated to slide on their linear tracks. The overall frame consisting of the three pairs of linear tracks form the skeleton which can be actuated in three rotational degrees of freedom (dof). (b) 2D Reaction wheel Pendulum Model. The distance between the two point masses is $2r$.

B. 2D Reaction wheel pendulum model

The 2D version of the RMP is equivalent to a reaction wheel pendulum, for which a realization is shown in Fig. 3(b). The generalized coordinates and generalized forces for this model are (θ, α, r_l, r) and $(\tau_\theta, \tau, f_l, f)$, respectively. The total mass of the pendulum is $0.5M + 0.5M = M$, whereas its rotational inertia about CoM is $\bar{I} = Mr^2$.

The equations of motion of this model are derived using Lagrangian techniques.

$$f_l = M\ddot{r}_l - Mr_l\dot{\theta}^2 + Mg \sin \theta \quad (10)$$

$$f = M\ddot{r} - Mr(\dot{\theta} + \dot{\alpha})^2 \quad (11)$$

$$\begin{aligned} \tau_\theta &= Mr_l^2\ddot{\theta} + Mr^2(\ddot{\theta} + \ddot{\alpha}) + 2Mr_l\dot{r}_l\dot{\theta} \\ &+ 2Mr\dot{r}(\dot{\theta} + \dot{\alpha}) + Mgr_l \cos \theta \end{aligned} \quad (12)$$

TABLE I
GENERALIZED VARIABLES OF RMP

Physical description	Generalized coordinates (forces)	
	2D	3D
Radial distances of three pairs of point masses forming the ellipsoid and their actuation on linear tracks	$r (f)$	r_1, r_2, r_3 (f_1, f_2, f_3)
Orientation angles of the ellipsoid body and their actuation	$\alpha (\tau)$	α, β, γ (τ_1, τ_2, τ_3)
Leg length and its actuation	$r_l (f_l)$	$r_l (f_l)$
Leg orientation angles and their actuation	$\theta (\tau_\theta)$	$\theta, \phi (\tau_\theta,$ $\tau_\phi)$
CoP position and ground reaction force	x_{CoP} (R_x, R_y)	$x_{CoP},$ y_{CoP} (R_x, R_y, R_z)

$$\tau = Mr^2(\ddot{\theta} + \ddot{\alpha}) + 2Mr\dot{r}(\dot{\theta} + \dot{\alpha}). \quad (13)$$

The ground reaction force to the reaction mass pendulum is $\mathbf{f}_r = M(\ddot{r}_l - \mathbf{g})$. We can also express the angular momentum in terms of the generalized coordinates; i.e., $\tau = \dot{\mathbf{k}}_G$ and $\tau_\theta = \dot{\mathbf{k}}_p + Mgr_l \cos \theta$.

As known, a reaction wheel pendulum can have interesting dynamics. For example, if we set $\tau_\theta = 0$, $\dot{\theta} = \ddot{\theta} = 0$, then we can compute τ that keeps $\theta = \theta_c$ stationary, i.e., $\tau = -Mgr \cos \theta_c$. The torque creates an angular acceleration $\ddot{\alpha}$ which cannot continue indefinitely due to robot joint limits. However, the example showcases the situation where the robot "leg" can be in static stability while the CoM ground projection is outside of the support base.

IV. INERTIA SHAPING: AN RMP-BASED CONTROLLER

A humanoid robot has a large number of DOFs: for example HOAP2 robot has 25 DOFs and Asimo has 27 DOFs. In order to kinematically transform an RMP back to a humanoid robot, one needs to generate a map from the 11-dimensional RMP space to the much larger robot kinematics space. A unique mapping will need additional constraints, such as in the form of desired hand or foot position.

For control purposes we need to string out the nonzero elements of a matrix. The "strung out" vector corresponding to the generalized inertia matrix is $\hat{\mathbf{I}} = (\hat{\mathbf{I}}^T, mr^T)^T \in \mathbb{R}^9$ and $\hat{\mathbf{I}} = (I_{xx}, I_{xy}, I_{xz}, I_{yy}, I_{yz}, I_{zz})^T$.

A. CRB inertia Jacobian

The CRB inertia Jacobian \mathbf{J}_I maps changes in the generalized coordinates into corresponding changes in the CRB inertia; i.e.,

$$\delta^s \hat{\mathbf{I}} = \mathbf{J}_I \delta \Theta. \quad (14)$$

In the following sections, we use \mathbf{I} in the spatial frame without using superscripts. The CRB inertia Jacobian is decomposed into two parts, $\mathbf{J}_I = [\mathbf{J}_{I,0} \mathbf{J}_{I,q}]$, where $\mathbf{J}_{I,0} \in \mathbb{R}^{9 \times 6}$ and $\mathbf{J}_{I,q} \in \mathbb{R}^{9 \times n}$ map the motion of the base frame and the joint angles, respectively, to the rate of change of the CRB inertia; i.e.,

$$\delta \hat{\mathbf{I}} = \mathbf{J}_{I,0} (T_0^{-1} \delta T_0) + \mathbf{J}_{I,q} \delta \mathbf{q}. \quad (15)$$

Specifically,

$$\begin{aligned} \mathbf{J}_{\mathbf{I},0} &= (J_{\mathbf{T}_{0,1}}, \dots, J_{\mathbf{T}_{0,6}}), \text{ where } J_{\mathbf{T}_{0,i}} = \dot{\hat{\mathbf{I}}}|_{\mathbf{v}_0=\mathbf{e}_i, \dot{\mathbf{q}}=0} \\ \mathbf{J}_{\mathbf{I},q} &= (J_{q_1}, \dots, J_{q_n}), \text{ where } J_{q_i} = \partial \hat{\mathbf{I}} / \partial q_i. \end{aligned}$$

Using the relations $\partial \text{Ad}_{\mathbf{G}_i} / \partial q_j = \text{Ad}_{\mathbf{G}_i} \text{ad}_{J_{i,j}}$ where $J_{i,j} = \mathbf{G}_i^{-1} \frac{\partial \mathbf{G}_i}{\partial q_j}$ as defined in (5), we can derive analytical expression for $\dot{\mathbf{I}}$ and $\frac{\partial \mathbf{I}}{\partial q_j}$; i.e.,

$$\dot{\mathbf{I}}|_{\dot{\mathbf{q}}=0} = -\text{ad}_{\mathbf{v}_0}^* \mathbf{I} - \mathbf{I} \text{ad}_{\mathbf{v}_0} \quad (16)$$

$$\frac{\partial \mathbf{I}}{\partial q_j} = -\sum_{i=1}^n \text{ad}_{J_{i,j}}^* \mathbf{I}_i + \mathbf{I}_i \text{ad}_{J_{i,j}}. \quad (17)$$

where another *adjoint mapping* $\text{ad}_{\mathbf{V}} : \text{se}(3) \rightarrow \text{se}(3)$ is given by $\text{ad}_{\mathbf{V}_1} \mathbf{V}_2 = \mathbf{V}_1 \mathbf{V}_2 - \mathbf{V}_2 \mathbf{V}_1$, or equivalently by

$$\text{ad}_{\mathbf{V}_1} \mathbf{V}_2 = \begin{bmatrix} [\mathbf{w}_1] & 0 \\ [\mathbf{v}_1] & [\mathbf{w}_1] \end{bmatrix} \begin{pmatrix} \mathbf{w}_2 \\ \mathbf{v}_2 \end{pmatrix}.$$

Note that the CRB inertia Jacobian includes the CoM Jacobian. If we partition $\mathbf{J}_{\mathbf{I}}$ into $\mathbf{J}_{\mathbf{I}} = [\mathbf{J}_{\mathbf{I}}^T \mathbf{J}_{\mathbf{G}}^T]^T$ where $\mathbf{J}_{\mathbf{G}}$ consists of the bottom 3 rows of $\mathbf{J}_{\mathbf{I}}$, we get

$$m\mathbf{r}_{\mathbf{G}} = \mathbf{J}_{\mathbf{G}} \dot{\Theta}. \quad (18)$$

$\mathbf{J}_{\mathbf{G}}$ maps the generalized velocity to the linear momentum of the system. In fact, it is the same as the CoM Jacobian scaled by the total mass.

B. CRB inertia Jacobian of humanoid

If the humanoid robot is not in contact with external environment, (15) completely describes the CRB inertia Jacobian. Otherwise, however, geometric constraints arise among the generalized coordinates, and it is advantageous to describe the CRB inertia Jacobian in independent coordinates.

Let us assume \mathbf{q} comprises of $\mathbf{q} = (q_r^T \ q_l^T \ q_t^T)^T$, where $\mathbf{q}_{\{r,l\}} \in \mathbb{R}^6$ is joint angles for right and left legs respectively and q_t is for the rest of joints. We also decompose $\mathbf{J}_{\mathbf{I}}$ accordingly; i.e.,

$$\mathbf{J}_{\mathbf{I}} = \begin{bmatrix} \mathbf{J}_{\mathbf{I}_0} & \mathbf{J}_{\mathbf{I}_r} & \mathbf{J}_{\mathbf{I}_l} & \mathbf{J}_{\mathbf{I}_t} \\ \mathbf{J}_{\mathbf{G}_0} & \mathbf{J}_{\mathbf{G}_r} & \mathbf{J}_{\mathbf{G}_l} & \mathbf{J}_{\mathbf{G}_t} \end{bmatrix}. \quad (19)$$

We describe CRB inertia Jacobian for each ground contact case.

1) Free floating:

$$\delta \hat{\mathbf{I}} = \mathbf{J}_{\mathbf{I}_0} (\mathbf{T}_0 \delta \mathbf{T}_0^{-1}) + [\mathbf{J}_{\mathbf{I}_r} \ \mathbf{J}_{\mathbf{I}_l} \ \mathbf{J}_{\mathbf{I}_t}] \delta \mathbf{q} \quad (20)$$

$$m\delta \mathbf{r}_{\mathbf{G}} = \mathbf{J}_{\mathbf{G}_0} (\mathbf{T}_0 \delta \mathbf{T}_0^{-1}) + [\mathbf{J}_{\mathbf{G}_r} \ \mathbf{J}_{\mathbf{G}_l} \ \mathbf{J}_{\mathbf{G}_t}] \delta \mathbf{q} \quad (21)$$

2) *Single support by left or right foot:* Let us suppose the humanoid robot is supported by one foot link, left foot link for example, which is stationary with respect to the ground. Then we can describe the constraint as follows;

$$\mathbf{T}_l^{-1} \delta \mathbf{T}_l = 0 \quad (22)$$

where \mathbf{T}_l is the transformation matrix for the left foot link. From $\mathbf{T}_l = \mathbf{T}_0 \mathbf{G}_l(\mathbf{q})$, we can derive the following relation;

$$\mathbf{T}_0^{-1} \delta \mathbf{T}_0 = -\text{Ad}_{\mathbf{G}_l} \mathbf{J}_l \delta \mathbf{q}. \quad (23)$$

Defining \mathbf{J}_l^* such that $\text{Ad}_{\mathbf{G}_l} \mathbf{J}_l \delta \mathbf{q} = \mathbf{J}_l^* \delta \mathbf{q}_l$, the CRB inertia Jacobian is written with respect to the joint angles;

$$\delta \hat{\mathbf{I}} = [\mathbf{J}_{\mathbf{I}_r} \ (\mathbf{J}_{\mathbf{I}_l} - \mathbf{J}_{\mathbf{I}_0} \mathbf{J}_l^*) \ \mathbf{J}_{\mathbf{I}_t}] \delta \mathbf{q} \quad (24)$$

$$m\delta \mathbf{r}_{\mathbf{G}} = [\mathbf{J}_{\mathbf{G}_r} \ (\mathbf{J}_{\mathbf{G}_l} - \mathbf{J}_{\mathbf{G}_0} \mathbf{J}_l^*) \ \mathbf{J}_{\mathbf{G}_t}] \delta \mathbf{q}. \quad (25)$$

3) *Double support:* When both feet are stationary to the ground, from the additional constraint $\mathbf{J}_l^* \delta \mathbf{q}_l = \mathbf{J}_r^* \delta \mathbf{q}_r$, we have $\delta \mathbf{q}_r = \mathbf{J}_r^{*-1} \mathbf{J}_l^* \delta \mathbf{q}_l$. Therefore,

$$\delta \hat{\mathbf{I}} = [(\mathbf{J}_{\mathbf{I}_l} + (\mathbf{J}_{\mathbf{I}_r} \mathbf{J}_r^{*-1} - \mathbf{J}_{\mathbf{I}_0}) \mathbf{J}_l^*) \ \mathbf{J}_{\mathbf{I}_t}] \begin{pmatrix} \delta \mathbf{q}_l \\ \delta \mathbf{q}_t \end{pmatrix} \quad (26)$$

$$m\delta \mathbf{r}_{\mathbf{G}} = [(\mathbf{J}_{\mathbf{G}_l} + (\mathbf{J}_{\mathbf{G}_r} \mathbf{J}_r^{*-1} - \mathbf{J}_{\mathbf{G}_0}) \mathbf{J}_l^*) \ \mathbf{J}_{\mathbf{G}_t}] \begin{pmatrix} \delta \mathbf{q}_l \\ \delta \mathbf{q}_t \end{pmatrix}. \quad (27)$$

C. Inertia shaping

An interesting application of our RMP modeling approach is what we call *inertia shaping* of an articulated chain. Inertia shaping is a high-level approach to precisely control the aggregate dynamic characteristics of an articulated chain by controlling its CRB inertia. Given a desired CRB inertia \mathbf{I}_d from the RMP model, the humanoid should make a proper pose to achieve this goal. This can be posed as an inverse kinematics problem with the desired CRB inertia constraints. Since we have derived the CRB inertia Jacobian, the inverse kinematics problem can be solved by any suitable optimization algorithm. The simplest solution will be updating desired joint angles using pseudo-inverse of CRB inertia Jacobian Eq. 14, i.e.,

$$\delta \Theta_{\mathbf{I}} = \mathbf{J}_{\mathbf{I}}^\dagger \delta (\hat{\mathbf{I}}_d - \hat{\mathbf{I}}) \quad (28)$$

where $\Theta_{\mathbf{I}}$ is the vector of independent generalized coordinates and $\mathbf{J}_{\mathbf{I}}^\dagger = \mathbf{J}_{\mathbf{I}}^T (\mathbf{J}_{\mathbf{I}} \mathbf{J}_{\mathbf{I}}^T)^{-1}$.

Fig. 4 presents three examples of inertia shaping on a non-contacting biped⁵ floating in space (say, a humanoid astronaut). The robot is given three different commands, shown in series *a*, *b*, and *c*, respectively, to try to match its own CRB inertia to a desired CRB inertia. Starting from an initial configuration, the robot moves its joints such that the cost function, the Frobenius norm of the difference between the two inertias, is minimized.

In Fig. 4(a) desired inertia components along all three axes are equal and large. Hence the robot tries to "expand" in all directions. In Fig. 4(b) the desired inertia along Y-axis (vertical) is big, and the other directions are very small. In Fig. 4(c) robot tries to make its inertia along X and Z larger at the cost of Y-direction.

This simulation demonstrates the important point of effectively controlling a complex biped with a very simple control law. While the robot model has 27 dofs, the control law deals with only three variables which are the three diagonal elements of the robot's rotational inertia.

⁵The biped is similar to the Honda humanoid Asimo with some simplifications.

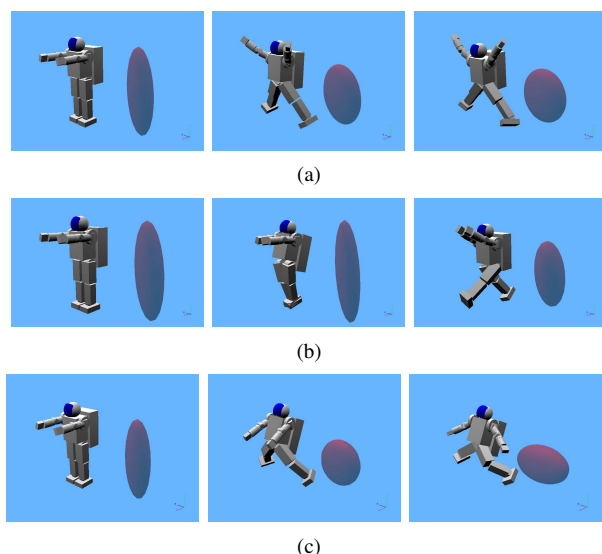


Fig. 4. Demonstration of the inertia shaping technique on a non-contacting biped robot floating in space. A floating robot has no CoP, so the RMP reduces to simply the ellipsoidal reaction mass.

V. CONCLUSIONS AND FUTURE WORK

We have introduced the reaction mass pendulum (RMP) model of a humanoid robot. The RMP model contains an actuated ellipsoidal reaction mass to explicitly model the robot's angular momentum. The ellipsoid represents the composite rigid body (CRB) inertia of the robot computed at its CoM. The reaction mass is an addition to the existing inverted pendulum humanoid models that only consider a point mass, and is also a mechanical realization of the AMPM model that accounts for the presence of centroidal angular momentum.

The RMP is an instantaneous 3D capture of the aggregate kinematics and dynamics of a general humanoid robot. As a lower-dimensional ($n = 11$) dynamic equivalent of a high-dof humanoid it lends itself to more probing analysis for dynamics and planning.

We presented the technique of inertia shaping, which can be thought of as a dynamics-based higher-level control for humanoid. We have provided detailed formulations for each ground contact configuration and demonstrated the successful application to a free floating case.

RMP is introduced mainly as an analysis tool. For it to be a worthwhile successor to the very useful linear inverted pendulum (LIPM) or AMPM models, one needs to formulate control laws based on linear or simplified dynamics of the RMP and apply them successfully to humanoids. This work is ongoing.

ACKNOWLEDGMENT

Sung-Hee wishes to thank Honda Research Institute for a summer internship. Ambarish appreciates fruitful discussions with Jerry Pratt, David Orin and especially with Stefano Stramigioli.

REFERENCES

- [1] S. Kajita, T. Yamaura, and A. Kobayashi, "Dynamic walk control of a biped robot along the potential energy conserving orbit," *IEEE Transactions on Robotics and Automation*, vol. 8, no. 4, pp. 431–438, 1992.
- [2] S. Kajita, F. Kanehiro, K. Kaneko, K. Fujiwara, K. Yokoi, and H. Hirukawa, "A realtime pattern generator for biped walking," in *IEEE International Conference on Robotics and Automation (ICRA)*, 2002, Washington, DC, pp. 31–37.
- [3] T. Sugihara and Y. Nakamura, "Variable impedant inverted pendulum model control for a seamless contact phase transition on humanoid robot," in *IEEE International Conference on Humanoid Robots (Humanoids2003)*, 2003.
- [4] T. Komura, A. Nagano, H. Leung, and Y. Shinagawa, "Simulating pathological gait using the enhanced linear inverted pendulum model," *IEEE Transactions on Biomedical Engineering*, vol. 52, no. 9, pp. 1502–1513, 2005, September.
- [5] M. Abdallah and A. Goswami, "A biomechanically motivated two-phase strategy for biped robot upright balance control," in *IEEE International Conference on Robotics and Automation (ICRA)*, April 2005, Barcelona, Spain, pp. 3707–3713.
- [6] S. Kajita, F. Kanehiro, K. Kaneko, K. Fujiwara, K. Harada, K. Yokoi, and H. Hirukawa, "Resolved momentum control: Humanoid motion planning based on the linear and angular momentum," in *IEEE/RSJ International Conference on Intelligent Robots and Systems*, 2003, Las Vegas, NV, USA, pp. 1644–1650.
- [7] J. Vermeulen, B. Verrelst, B. Vanderborght, D. Lefeber, and P. Guillaume, "Trajectory planning for the walking biped."
- [8] R.M. Murray, Z.X. Li, and S.S. Sastry, *A Mathematical Introduction to Robotic Manipulation*, CRC Press, 1994.
- [9] J. Ostrowski, "Computing reduced equations for robotic systems with constraints and symmetries," *IEEE Transactions on Robotics and Automation*, vol. 15, no. 1, pp. 111–123, 1999.
- [10] S. H. Crandall, D. Karnopp, E. F. Kurtz, and D. C. Pridmore-Brown, *Dynamics of Mechanical and Electromechanical Systems*. Malabar, FL: Krieger Publishing Company, 1982.
- [11] F. P. Beer and E. R. Johnson, *Vector Mechanics for Engineers: Dynamics*. New York: McGraw-Hill Book Company, 1984.
- [12] Webots, *commercial Mobile Robot Simulation Software*. [Online]. Available: <http://www.cyberbotics.com>
- [13] P. Cominoli, "Development of a physical simulation of a real humanoid robot," Master's thesis, Swiss Federal Institute of Technology (EPFL), Lausanne, 2005.
- [14] M. J. Sidi, *Spacecraft Dynamics and Control*. New York, NY: Cambridge University Press, 1997.
- [15] K. Astrom, A. Block, and M. Spong, *The Reaction Wheel Pendulum*, L. Notes, Ed. Downloadable from: <http://decision.csl.uiuc.edu/~spong/main.htm>, 2001.
- [16] R. Olfati-Saber, "Stabilization of a flat underactuated system: the inertia wheel pendulum," in *40th Conference on Decision and Control*, December 4-7 2001, Orlando, FL, pp. 306–308.
- [17] M. W. Spong, P. Corke, and R. Lozano, "Nonlinear control of inertia wheel pendulum," *Automatica*, vol. 37, pp. 1845–1851, February 2001.
- [18] A. Kuo, "Stabilization of lateral motion in passive dynamic walking," *International Journal of Robotics Research*, vol. 18, no. 9, pp. 917–930, 1999, September.
- [19] J. Pratt, "Exploiting inherent robustness and natural dynamics in the control of bipedal walking robots," Ph.D. dissertation, MIT, PhD Thesis, 2000.
- [20] T. Komura, H. Leung, S. Kudoh, and J. Kuffner, "A feedback controller for biped humanoids that can counteract large perturbations during gait," in *IEEE International Conference on Robotics and Automation (ICRA)*, 2005, Barcelona, Spain, pp. 2001–2007.
- [21] N. M. Mayer, F. Farkas, and M. Asada, "Balanced walking and rapid movements in a biped robot by using a symmetric rotor and a brake," in *International Conference on Mechatronics and Automation*, July 29- August 1, 2005 2005, Niagara Falls, Ontario, Canada.
- [22] M. W. Walker and D. Orin "Efficient dynamic computer simulation of robotic mechanisms" in *ASME Journal of Dynamic Systems, Measurement, and Control*, Vol. 104, pp. 205-211, Sept 1982